Journal of Zhejiang University-SCIENCE B (Biomedicine & Biotechnology) 2022 23(4):315-327
www.jzus.zju.edu.cn; www.springer.com/journal/11585
E-mail: jzus_b@zju.edu.cn

Research Article

https://doi.org/10.1631/jzus.B2100877

Check for updates

# *Toxoplasma gondii* infection induces cell apoptosis via multiple pathways revealed by transcriptome analysis

Kaige DU[1,2], Fei LU[1], Chengzuo XIE[1], Haojie DING[1], Yu SHEN[1], Yafan GAO[1], Shaohong LU[1]✉, Xunhui ZHUO[1]✉

[1]*School of Basic Medical Sciences and Forensic Medicine, Hangzhou Medical College, Hangzhou 310053, China*
[2]*Shandong Center for Disease Control and Prevention, Jinan 250021, China*

**Abstract:** *Toxoplasma gondii* is a worldwide parasite that can infect almost all kinds of mammals and cause fatal toxoplasmosis in immunocompromised patients. Apoptosis is one of the principal strategies of host cells to clear pathogens and maintain organismal homeostasis, but the mechanism of cell apoptosis induced by *T. gondii* remains obscure. To explore the apoptosis influenced by *T. gondii*, Vero cells infected or uninfected with the parasite were subjected to apoptosis detection and subsequent dual RNA sequencing (RNA-seq). Using high-throughput Illumina sequencing and bioinformatics analysis, we found that pro-apoptosis genes such as DNA damage-inducible transcript 3 (*DDIT3*), growth arrest and DNA damage-inducible α (*GADD45A*), caspase-3 (*CASP3*), and high-temperature requirement protease A2 (*HtrA2*) were upregulated, and anti-apoptosis genes such as poly(adenosine diphosphate (ADP)-ribose) polymerase family member 3 (*PARP3*), B-cell lymphoma 2 (*Bcl-2*), and baculoviral inhibitor of apoptosis protein (IAP) repeat containing 5 (*BIRC5*) were downregulated. Besides, tumor necrosis factor (TNF) receptor-associated factor 1 (*TRAF1*), *TRAF2*, TNF receptor superfamily member 10b (*TNFRSF10b*), disabled homolog 2 (DAB2)-interacting protein (*DAB2IP*), and inositol 1,4,5-trisphosphate receptor type 3 (*ITPR3*) were enriched in the upstream of TNF, TNF-related apoptosis-inducing ligand (TRAIL), and endoplasmic reticulum (ER) stress pathways, and TRAIL-receptor 2 (TRAIL-R2) was regarded as an important membrane receptor influenced by *T. gondii* that had not been previously considered. In conclusion, the *T. gondii* RH strain could promote and mediate apoptosis through multiple pathways mentioned above in Vero cells. Our findings improve the understanding of the *T. gondii* infection process through providing new insights into the related cellular apoptosis mechanisms.

**Key words:** *Toxoplasma gondii*; Transcriptome analysis; Apoptosis; Infection

## 1 Introduction

*Toxoplasma gondii* is a worldwide protozoan that infects over 30% of the human population (Parlog et al., 2015). This parasite can also affect animals like cats, pigs, and goats, leading to considerable medical concerns in addition to veterinary and economic losses (Zhuo et al., 2017). The three major strain types, namely, types I, II, and III of *T. gondii* differ regarding their virulence, propagation, and pathogenicity. The type I strain of high virulence, such as RH strain and GT1 strain, could cause acute and fatal infections in immunocompromised patients; the type II of low virulence consistently results in chronic infection; type III is avirulent (Fox and Bzik, 2015). *T. gondii* is an obligatory parasite with complex organelles specialized for the invasion of and movement within host cells, and it resides in parasitophorous vacuole membrane (PVM) to escape host immune response. Polymorphic secreted effectors released from this parasite can manipulate gene expression and host cell disorder signaling pathways to establish life-long infection (Venugopal and Marion, 2018).

Cell apoptosis is one of the important defense mechanisms against infection by intracellular pathogens. It is a programmed death response to remove damaged cells and keep host homeostasis closely associated with cell replication, proliferation, immunity, and cancer; however, excessive apoptosis may cause disease (Lin et al., 2018; Mammari et al., 2019; Rajedadram et al., 2021). Previous studies have demonstrated that

✉ Xunhui ZHUO, zhuoxh@zjams.com.cn
Shaohong LU, lsh@zjams.com.cn
Xunhui ZHUO, https://orcid.org/0000-0001-5805-0711
Shaohong LU, https://orcid.org/0000-0001-9855-7154

Received Oct. 14, 2021; Revision accepted Jan. 16, 2022;
Crosschecked Mar. 1, 2022

apoptotic genesis is dependent on the host cell type and *T. gondii* strain involved; multiple proteins and pathways have been found to participate in apoptosis and act as important targets modulated by *T. gondii*. For instance, rhoptry protein 18 (ROP18) of the RH strain has been reported to promote apoptosis in mouse neuroblastoma Neuro2a cells (Wan et al., 2015), but inhibit apoptosis in human SF268 neural cells and 293T cells (Zhou et al., 2019). In mice splenocytes, the *T. gondii* RH strain inhibited apoptosis, while ME49 strain promoted it (Quan et al., 2013). Some researchers have confirmed that high-virulence *Toxoplasma* can decrease the expression of anti-apoptotic protein B-cell lymphoma 2 (Bcl-2) and cell survival, and increase the expression of pro-apoptotic proteins caspase-3 (CASP3) and C/EBP-homologous protein (CHOP) in mouse cells (Wang et al., 2014). However, the type I strain can also inhibit host cell apoptosis by inducing the expression of anti-inflammatory cytokines and increasing extracellular regulated protein kinase (ERK) protein phosphorylation in human trophoblastic cells (Angeloni et al., 2013). The apoptosis-associated signaling pathways are also modulated differently when infected with various strains. ROP16 from type I and type III is responsible for activating the signal transducer and activator of transcription (STAT) signaling pathway (Rosowski and Saeij, 2012), while dense granule protein 15 (GRA15) of type II mediates nuclear factor κB (NF-κB) activation (Rosowski et al., 2011). Therefore, it seems difficult to conclude the clear mechanism of cell apoptosis induced by *T. gondii*. Previous studies have mainly focused on some particular or few molecular targets on apoptosis. However, the integral apoptosis-associated gene changes in host cells were neglected, and the effect induced by *T. gondii* recombinant protein alone in some experiments may be quite different from that induced by the whole parasite (Wei et al., 2018). In addition, a previous study demonstrated that the transcripts of mouse peritoneal cells were similar after infection with type I and type II *T. gondii* strains, and both showed greater changes than those infected with type III strain (Hill et al., 2012).

To explore apoptotic processes influenced by *T. gondii* as well as the apoptosis-related gene expression and signaling pathways involved in the host–parasite interaction, apoptosis detection and RNA sequencing (RNA-seq) were performed on the infected Vero cells and uninfected cells. The gene expression profile and differentially expressed genes (DEGs) were investigated by cell transcriptome analysis. The detection results and RNA-seq data demonstrated the promotive effect of *T. gondii* on apoptosis in Vero cells, which uncovered the basis of apoptosis regulation and could provide novel information of the potential mechanism for future research (Cong et al., 2018).

## 2 Materials and methods

### 2.1 Preparation of *T. gondii* tachyzoites and Vero cells

Vero cells were cultured in Dulbecco's modified Eagle medium (DMEM; Gibco, Thermo Fisher Scientific Inc., Waltham, MA, USA) nutrient solution supplemented with 5% (volume fraction) fetal bovine serum (FBS; Gibco), penicillin (100 U/mL, Life Technologies, Gaithersburg, MD, USA), and streptomycin (100 μg/mL, Life Technologies) at 37 °C in an incubator under 5% $CO_2$. Tachyzoites of the RH strain of *T. gondii* were maintained in Vero cells.

### 2.2 In vitro infection

After culture in the Vero cells for 3–4 generations, the freshly egressed tachyzoites were passed through 25-gauge (25G) needles and then purified by a 5-μm filter. The tachyzoites were counted and then subjected to Vero cells at a multiplicity of infection (MOI) value of 3:1. The infected and uninfected cells were cultured under the same conditions as described above (Cui and Shen, 2020).

### 2.3 Detection of apoptotic phenotype

The apoptosis of Vero cells induced by *T. gondii* infection was detected by a Becton-Dickinson FACSCalibur flow cytometer (Becton Dickinson, San Jose, CA, USA). Vero cells ($0.5\times10^6$–$1.0\times10^6$) were seeded into a six-well cell plate and infected with *T. gondii* tachyzoites (MOI=3:1) for 12 or 24 h. The Vero cells were then stained with fluorescence isothiocyanate (FITC)-conjugated Annexin V and propidium iodide (PI) using the instructions of the apoptotic detection kit (Beyotime, China). Briefly, the Vero cells were washed twice with phosphate-buffered saline (PBS), and added with 195 μL Annexin V-FITC-binding buffer, 5 μL Annexin V-FITC

reagent, and 10 μL PI dye. The samples were then evaluated with the flow cytometer, and data processing was carried out using FlowJo-V10 software (Becton Dickinson, USA).

### 2.4 RNA extraction and qualification

After being infected with *T. gondii* under the same conditions as described previously, the total RNA was extracted using TRIzol® Reagent (Invitrogen, Carlsbad, CA, USA) according to manufacturer's protocol. Two replication experiments were performed, in which Vero cells were infected or uninfected with *T. gondii* for 24 h. The RNA quality and concentration were checked by a Nanodrop 2000 device (Thermo Scientific Inc., Wilmington, DE, USA), and RNA integrity was determined by an Aglient 2100 BioAnalyzer (Agilent Technologies, Santa Clara, CA, USA). The samples that met the quality control requirements (standard RNA 28S/18S ratio of ⩾1.5 and integrity number of ⩾8.0) were selected for RNA-seq.

### 2.5 Transcriptome sequencing and alignment reading

The messenger RNA (mRNA) was enriched by binding to magnetic beads with oligonucleotide attachment, and then fragmented for complementary DNA (cDNA) synthesis. The cDNA was prepared for polymerase chain reaction (PCR) amplification and construction of sequence libraries, followed by steps of purification, repairing blunt ends, and adding adaptor to 3'-ends. As soon as the library quality assessment was up to the required standard, the sequencing was performed on an Illumina Novaseq™ 6000 platform (LC Sciences, Houston, Texas, USA), with read length of 150 bp paired-end. After removing the adaptors by Cutadapt (Version 1.9; https://cutadapt.readthedocs.io/en/stable) and verifying the quality of sequence through the FastQC program (Version 0.11.9; https://www.bioinformatics.babraham.ac.uk/projects/fastqc), the clean reads were mapped to the genome of *Chlorocebus sabaeus* (International Nucleotide Sequence Database Collaboration (INSDC): JACDXN000000000.1) by using HISAT2 (Version 2.0.4; https://daehwankimlab.github.io/hisat2), followed by assembling the reads and calculating reads per kilobase per million mapped reads (RPKMs) via StringTie (Version 2.1.4; https://ccb.jhu.edu/software/stringtie). The gene expression value that meets fragments per kilobase per million (FPKMs) of ⩾10 was utilized for further analysis.

### 2.6 Gene expression level and differential expression analyses

The edgeR Bioconductor package (Version 3.14.0; https://bioconductor.org/packages/release/bioc/html/edgeR.html) was used to identify DEGs and visualize the gene expression profiles. The threshold of significant DEGs was adjusted as $P<0.01$ and $|\log_2(\text{fold change})|>1$ (Zhou et al., 2016). The Gene Ontology (GO) Version 2019.5 and Kyoto Encyclopedia of Genes and Genomes (KEGG) Version 2019.5 databases were used to identify the biological functions of DEGs and the overrepresented biological processes of infected cells. The Search Tool for Retrieval of Interacting Genes/Proteins (STRING; https://www.string-db.org) database was employed to explore the information on protein–protein interaction (PPI) of apoptosis-associated DEGs, and the required confidence score of PPI network was chosen as ⩾0.4 (Szklarczyk et al., 2015). Hub gene screening was performed using cytoHubba, a plugin of Cytoscape software (Version 3.7.1; https://cytoscape.org) (Bader and Hogue, 2003). All of the DEGs enriched in the apoptosis pathway were counted and ranked by the maximal clique centrality (MCC), a topological analysis method, to improve the precision of predicting essential proteins from the yeast PPI network (Chin et al., 2014).

### 2.7 Gene expression validation by qRT-PCR

To verify the authenticity of gene expression trend induced by *T. gondii*, the extracted RNA templates were reversely transcribed to cDNA through reverse transcriptase (TOYOBO, Japan) and quantitative real-time PCR (qRT-PCR). The 20-μL reaction mixture contained SYBR Green I Master Mix (TOYOBO) with special primers (Table 1) was performed on a CFX-Manager real-time system (Bio-Rad, USA). The $2^{-\Delta\Delta C_T}$ method was used to calculate the relative gene expression as previously reported (Livak and Schmittgen, 2001). Three independent replicate experiments were carried out.

### 2.8 Statistical analysis

The GO and KEGG pathway enrichment analyses were performed by Fisher's exact test, and the *P*-value was corrected by the *Q*-value. The gene expression differences between the infected and uninfected groups were evaluated by independent-samples *t*-test.

**Table 1 Primers for qRT-PCR**

| Gene | Primers | Product length (bp) |
|---|---|---|
| *TRAF1* | F: 5'-CTCTTCTCCCCAGCCTTCTAC-3'<br>R: 5'-CAGCAACGCATCATACTCCC-3' | 141 |
| *DDIT* | F: 5'-ACCTCCTGGAAATGAAGAGGAAG-3'<br>R: 5'-TGTGACCTCTGCTCGTTCTG-3' | 103 |
| *GADD45A* | F: 5'-AGCAGAAGACCGAAAGGATGG-3'<br>R: 5'-GCACAACACCACGTTATCGG-3' | 143 |
| *CASP3* | F: 5'-TGGAAGCAAATCAGTGGACTCT-3'<br>R: 5'-ACCGAGATGCCATTCCAGTG-3' | 128 |
| *ATF3* | F: 5'-AAGAGGCGGCGAGAAAGAAAT-3'<br>R: 5'-AGCTTCTCTGACTCTTTCTGCA-3' | 95 |
| *AIFM1* | F: 5'-GCCACAGAGCAGTCAGGAAC-3'<br>R: 5'-TGACACCTTTGCCGTAGTCC-3' | 136 |
| *LAMN* | F: 5'-GGCTGCGTAACAAGTCCAAT-3'<br>R: 5'-TGCAGCCCAGATCGTTACC-3' | 143 |
| *BIRC5* | F: 5'-CTCAAGGACCACCGCATCTC-3'<br>R: 5'-GCCAAGTCTGGCTCGTTCT-3' | 125 |
| *IL12A* | F: 5'-CACGCTTCAGAAGGCCAGACA-3'<br>R: 5'-AATTCCAATGGTAAACAGGCCTCT-3' | 120 |
| *IL1A* | F 5'-GACCTTCAAGCAGAGCATGG-3'<br>R: 5'-GACCTGGGCTTGATGATTTCTTC-3' | 144 |
| *IL6* | F: 5'-ACATGTGTGAAAGCAGCAAAGAG-3'<br>R: 5'-TCACCAGGCAAGTCTCCTCAT-3' | 114 |
| *CCL20* | F: 5'-ACATCAATGCTGTCATCTTTCACA-3'<br>R: 5'-AATCAATTTCACCCAGGTCTGC-3' | 80 |
| *CXCL8* | F: 5'-AGCTCTGTGTGAAGGTGCAGTT-3'<br>R: 5'-CAGTGTGGTCCACTCTCAATCA-3' | 132 |
| *RPS18* | F: 5'-AAATAGCCTTTGCCATCACTGC-3'<br>R: 5'-TGATCACACGTTCCACCTCATC-3' | 132 |
| *GAPDH* | F: 5'-AAGGTCGGAGTCAACGGATTT-3'<br>R: 5'-ATGGGTGGAATCATACTGGAACA-3' | 147 |

qRT-PCR: quantitative real-time polymerase chain reaction; F: forward; R: reverse.

A $P$-value of <0.05 was considered as statistically significant.

## 3 Results

### 3.1 Effect of *T. gondii* on Vero cell apoptosis

We observed that the early apoptotic cells infected with *T. gondii* tachyzoites increased significantly compared with control cells. As revealed by flow cytometry, the rates of early and late apoptotic cells of the control group were about 2.99% and 2.40%, respectively, while in those infected with *T. gondii*, the early and late apoptotic cells reached 72.30% and 7.53% for 12 h and 64.80% and 11.59% for 24 h, respectively (Fig. 1). These results showed that *T. gondii* could induce apoptosis in the early stage in the infected group compared with the negative control group.

### 3.2 General features of the transcriptome data

After removing the adaptor and low-quality reads, 160 million clean reads were acquired, which accounted for nearly 80% of the total reads. Each sample had at least 97% clean reads that reached the Phred Quality score of 30 (Q30), and the GC content was about 48%, representing a high-level quality of the sequenced bases. In the infection groups, an average of 57% clean reads could be uniquely mapped to reference genomes, and the sites of approximately 85% of mapped sequences were within exons (Table 2).

### 3.3 Effect of *T. gondii* infection on gene expression profiles in Vero cells

In order to identify the Vero cell's DEGs infected by *T. gondii*, genes with the corrected FPKM value greater than 10 was regarded as expressed genes.

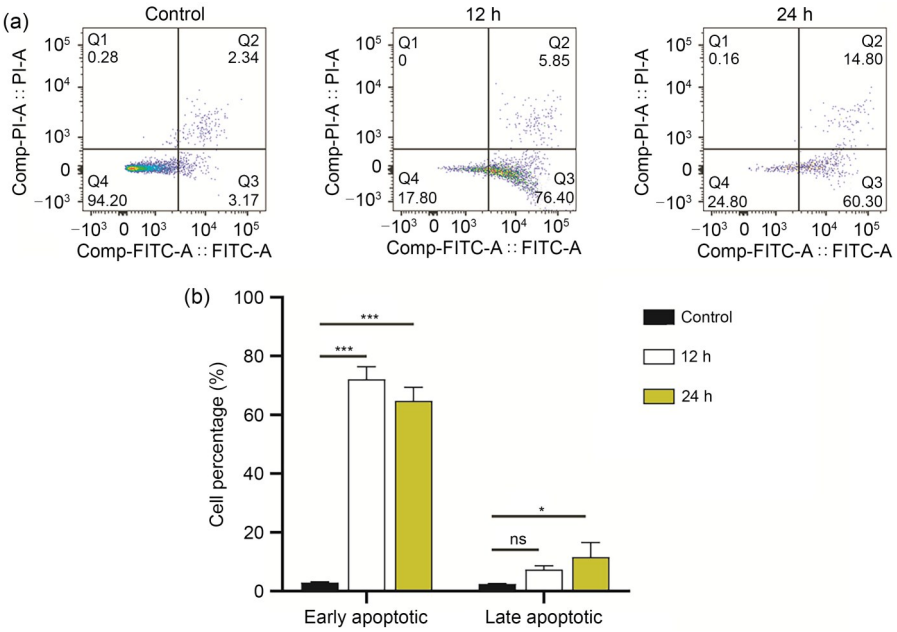


**Fig. 1 Flow cytometry analyses of Vero cells infected with *Toxoplasma gondii*. Vero cells were infected with *T. gondii* tachyzoites (MOI=3:1) at 12 or 24 h post-infection. (a) Cells were determined as live ($FITC^-/PI^-$), early apoptotic ($FITC^+/PI^-$), late apoptotic ($FITC^+/PI^+$), and necrotic ($FITC^-/PI^+$) depending on staining. (b) Comparison of cells between different groups. Data are expressed as mean±standard deviation (SD) of three independent tests. ns: not significant; * $P<0.05$; *** $P<0.001$. MOI: multiplicity of infection; FITC: fluorescence isothiocyanate; PI: propidium iodide.**

**Table 2 Distribution of sequencing data**

| Sample | Valid data | | Valid ratio (%) | Q30 (%) | GC content (%) | Number of reads* | | | Exon (%) |
|---|---|---|---|---|---|---|---|---|---|
| | Read | Base (Gb) | | | | Mapped | Unique mapped | Multi-mapped | |
| Ctrl1 | 41 047 806 | 6.16 | 80.63 | 97.88 | 48.50 | 39 064 606 (95.17%) | 29 344 754 (71.49%) | 9 719 852 (23.68%) | 85.31 |
| Ctrl2 | 42 838 750 | 6.43 | 78.45 | 98.02 | 48.00 | 41 062 033 (95.85%) | 30 843 666 (72.00%) | 10 218 367 (23.85%) | 85.77 |
| T.g1 | 39 040 728 | 5.86 | 81.19 | 97.94 | 49.00 | 29 830 596 (76.41%) | 22 292 307 (57.10%) | 7 538 289 (19.31%) | 84.88 |
| T.g2 | 37 745 558 | 5.66 | 80.72 | 97.97 | 49.50 | 28 665 634 (75.94%) | 21 512 741 (56.99%) | 7 152 893 (18.95%) | 85.29 |

* Data are expresses as number (percentage). A read: an inferred sequence of base pairs corresponding to all or part of a single DNA fragment. Q30: Phred Quality score of 30 (rate of incorrect base sequencing is less than 0.001); Ctrl: control; T.g: *Toxoplasma gondii*.

Among the expressed genes, those with the $\log_2$(fold-change) of gene expression value of >1 or <−1 and adjusted *P*-value of <0.01 were regarded as DEGs. Under these requirements, the screening resulted in 1579 DEGs, of which 918 genes were upregulated and 661 genes were downregulated (Fig. 2). Among the DEGs, 27 genes related to apoptosis were significantly expressed, including 16 upregulated and 11 downregulated genes.

### 3.4 GO analysis

GO is an international standard to classify genes into various biological functions. After GO analysis for DEGs, 1579 genes obtained functional annotations and were significantly enriched in biological process, cellular component, and molecular function. The top three GO terms, including microtubule binding, nucleus, and negative transcription regulation, were significantly different between *T. gondii*-infected and mock-infected control groups (Figs. 3 and 4).

### 3.5 KEGG analysis

The KEGG analysis represents pathways with known functions (Lu et al., 2019). The results of KEGG analysis showed that 54 pathways were enriched, with the pathway in cancer being the most significant one. Others within the top 10 significant pathways were involved in virus infection, axon guidance, cancer, and cell senescence (Fig. 5).

### 3.6 Gene expression changes in the apoptosis signaling pathway

Among DEGs in the apoptosis signaling pathway, most of the upregulated genes belonged to pro-apoptosis genes, such as DNA damage-inducible transcript 3 (*DDIT3*), growth arrest and DNA damage-inducible α (*GADD45A*), *CASP3*, and high-temperature requirement protease A2 (*HtrA2*), and most of the down-regulated genes were anti-apoptosis, such as poly(adenosine diphosphate (ADP)-ribose) polymerase family member 3 (*PARP3*), *Bcl-2*, and baculoviral inhibitor of apoptosis protein (IAP) repeat-containing 5 (*BIRC5*) (Fig. 6). The apoptosis signaling pathway map including DEGs was shown in Fig. 7. The PPI network of apoptosis-associated genes and the hub gene showed that *CASP3* was the top hub gene with the most interactions (Fig. 8).

The result of RNA-seq was confirmed by qRT-PCR. Fifteen genes were randomly selected from the apoptosis pathway and immune-related pathways. The gene expression was normalized to *RPS18* as a reference gene, and the data were represented as mean

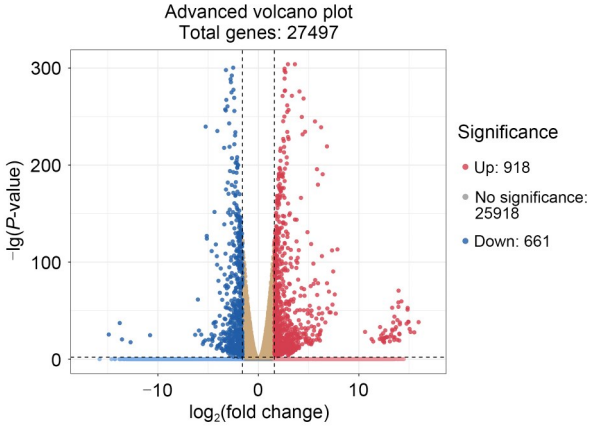


**Fig. 2 Volcano plot of DEGs between the infected and the control groups. The red and blue dots represent significant differential genes at adjusted *P*-value<0.01 and $|\log_2(\text{fold change})|>1$. The brown dots represent no significant genes in the infected group vs. the control group. DEG: differentially expressed gene.**

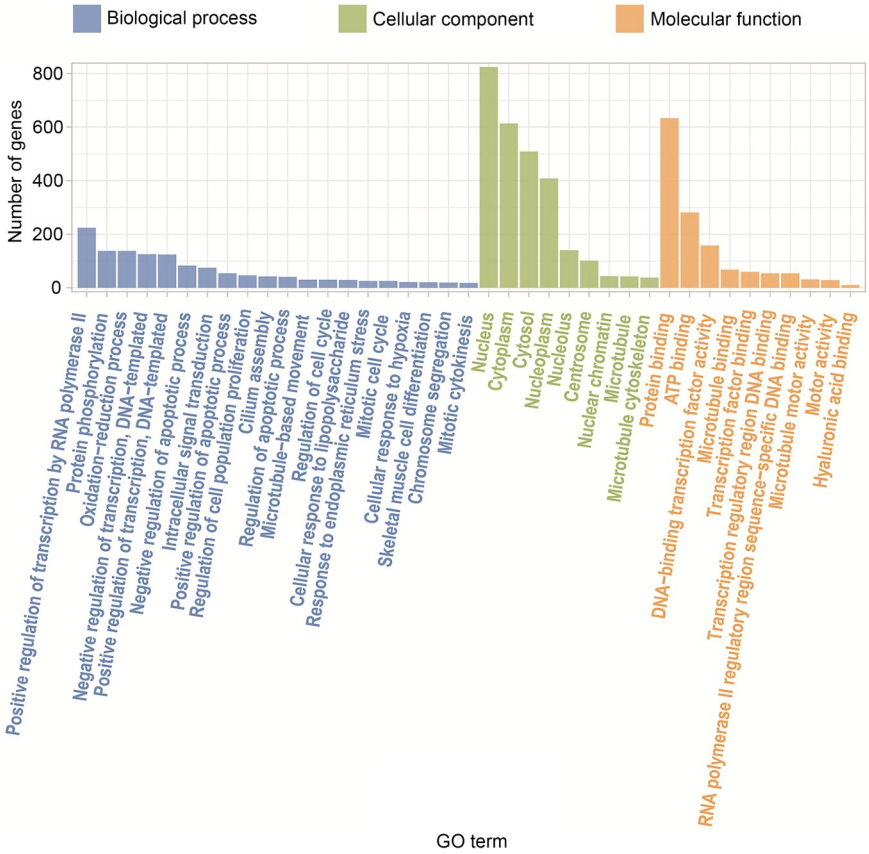


**Fig. 3 GO enrichment of DEGs. The *X*-axis represents the significant GO terms divided into molecular function, cellular component, and biological process. The *Y*-axis represents the number of DEGs enriched in the term. GO: Gene Ontology; DEG: differentially expressed gene.**

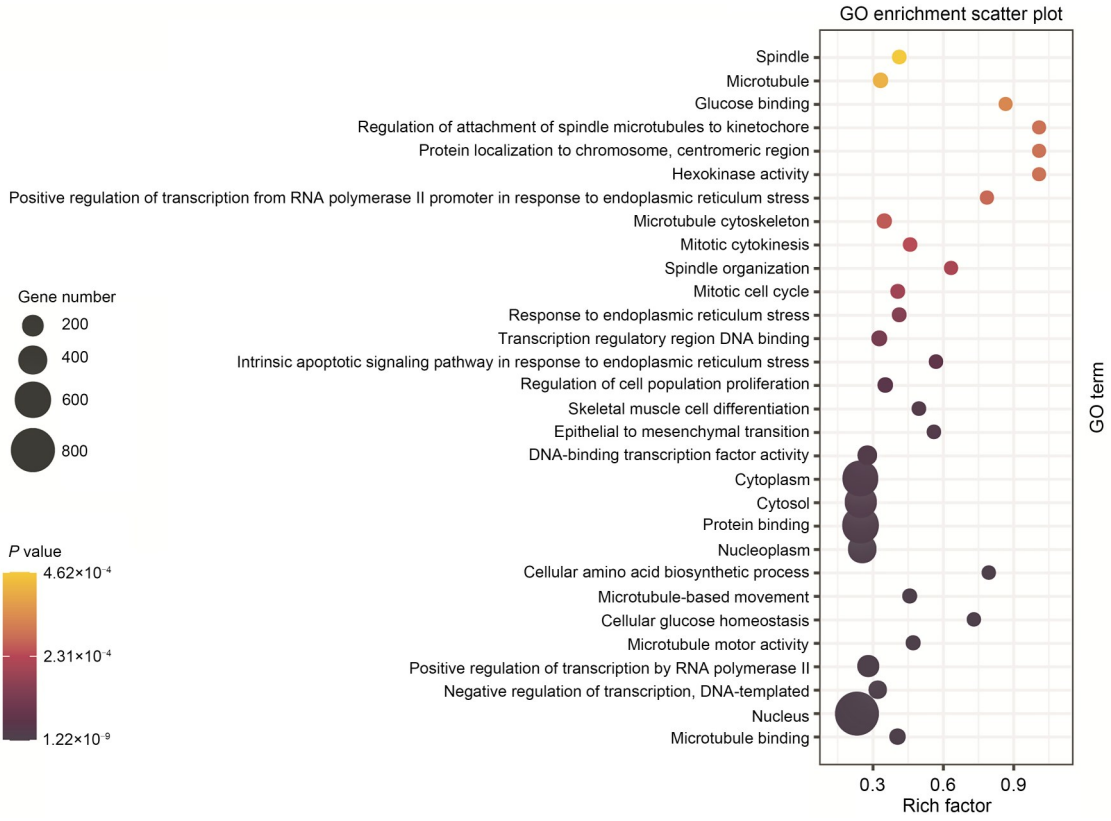


**Fig. 4 GO enrichment analysis of DEGs in the infected group compared with the control group. The most significant GO terms were those with corrected *P*-value of <0.05. The rich factor represents the number of DEGs that exist in this term accounting for the total number of genes of this term. GO: Gene Ontology; DEG: differentially expressed gene.**

value±standard error of mean (SEM). Linear correlation analysis with $r$=0.976 meant that the qRT-PCR results were nearly consistent with RNA-seq data (Fig. 9).

## 4 Discussion

Toxoplasmosis has been considered as a serious public health issue, and studies on the interaction between *T. gondii* and host cells can provide theoretical suggestions for treatment and prevention. *T. gondii* has been reported to change the gene expression and transcription profiles of host cells; however, few studies have focused on the expression of apoptosis-related genes and pathways. Therefore, based on the observed phenomenon of apoptotic genesis, Vero cells were sequenced and the comparative analysis of gene expression was undertaken comparing infected and uninfected groups, in order to identify the significant genes and molecular apoptosis pathways for an in-depth knowledge about host–parasite interactions.

Overall, 1579 DEGs enriched to 54 distinct pathways were characterized and identified. Unsurprisingly, apoptosis pathways were significantly regulated among these pathways. The classic apoptosis signaling pathways include the membrane receptor pathway and the mitochondria pathway (Lima and Lodoen, 2019), and overwhelming endoplasmic reticulum (ER) stress signal also promotes apoptosis (Ariyasu et al., 2017). In the apoptosis signaling pathway, 27 genes were significantly expressed, including 16 upregulated and 11 downregulated genes. Most upregulated genes were pro-apoptosis, such as *DDIT3*, *GADD45A*, *CASP3*, and *HtrA2*, and most downregulated genes were anti-apoptosis, such as *Bcl-2*, *PARP3*, and *BIRC5*.

Among the upregulated genes, tumor necrosis factor (TNF) receptor-associated factor 1 (*TRAF1*) was the most significant one, and *TRAF2* was also upregulated. TRAFs are intracellular adaptors that bind to TNF receptor-associated death domain (TRADD) and act in several pathways involved in apoptosis regulation, cell death, immunity, inflammation, cancer, etc.

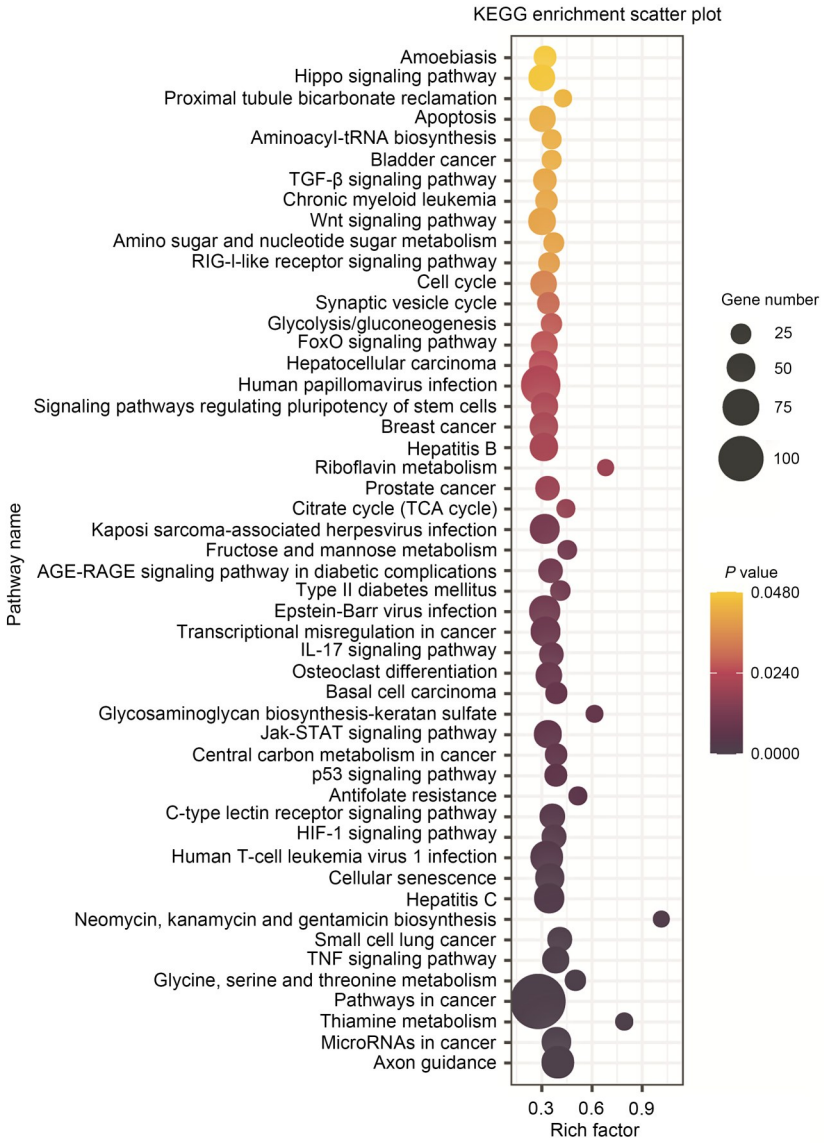


**Fig. 5 KEGG pathway enrichment analyses of DEGs. The top 50 pathways with corrected *P*-value of <0.05 were considered the significant pathways, and these were presented. The rich factor represent DEG number accounting for the total number of genes of this pathway. KEGG: Kyoto Encyclopedia of Genes and Genomes; DEG: differentially expressed gene.**

(Sajjad et al., 2019; Kim and Park, 2020). Furthermore, the genes expressing TRAF2-interacting proteins, including receptor-interacting serine/threonine kinase 1 (*RIPK1*), disabled homolog 2 (DAB2)-interacting protein (*DAB2IP*), and endoplasmic reticulum to nucleus signaling 1 (*ERN1*), were also upregulated. All the above-mentioned genes were enriched in the upstream of TNF and ER stress pathways, and their common downstream signal was the apoptosis signal-regulating kinase 1 (ASK1)-c-Jun N-terminal kinase (JNK) pathway. This implied that *T. gondii* could mediate apoptosis through the TNF and ER stress pathways, then via the ASK1-JNK pathway, and finally act on mitochondria (Fig. 7). Furthermore, the upregulation of TNF receptor superfamily member 10b (*TNFRSF10b*) revealed that another membrane receptor pathway was also affected. The *TNFRSF10b* expresses membrane receptor TNF-related apoptosis-inducing ligand-receptor (TRAIL-R), which interacts with extracellular protein TRAIL and recruits intracellular protein Fas-associated protein with death domain (FADD), and then it triggers the caspase cascade leading to apoptosis (Yuan et al., 2018). Thus far, few studies have focused on the TRAIL pathway in *T. gondii* infection;

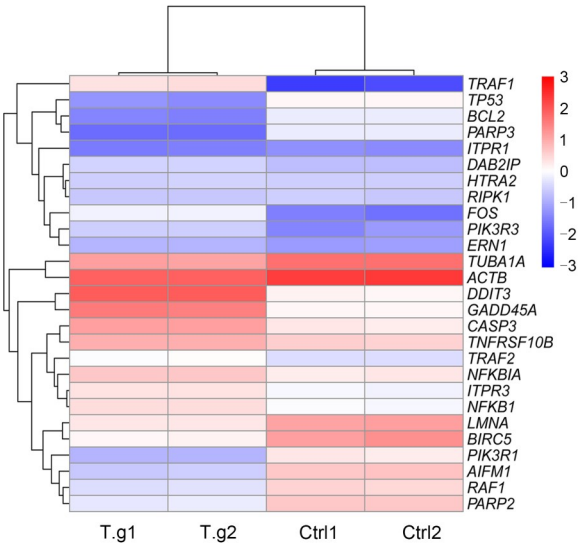


**Fig. 6 Heatmap of DEGs in the apoptosis pathway. The gradient color represents the expression level (FPKMs) of genes. The expression level was $\log_2$-transformed and median-centered. The vertical axis represents DEGs' clusters, and the horizontal axis represents the clusters of infected and control groups. DEG: differentially expressed gene; FPKMs: fragments per kilobase per million. T.g: *Toxoplasma gondii*; Ctrl: control.**

however, the important role of FADD and its close relationship with other proteins shown by the PPI network require further investigation.

*CASP3* is a hub gene in the apoptosis pathway, playing a pivotal role in apoptotic execution (Lossi et al., 2018). It could activate deoxyribonuclease and destruct lamin, resulting in DNA fragmentation, nuclear protein degradation, and cell proliferation inhibition (Estaquier et al., 2012). It also hydrolyzes anti-apoptosis proteins such as IAP, PARP, and Bcl-2 to promote apoptosis (Enari et al., 1998). Based on the sequencing data, *CASP3* was upregulated, and the genes *PARP2*, *PARP3*, *BIRC5*, *Bcl-2*, lamin A (*LMNA*), tubulin α-1A (*TUBA1A*) and β-actin (*ACTB*), expressing proteins hydrolyzed by *CASP3*, were downregulated, which indicated that the pro-apoptosis factors were increased and anti-apoptosis factors were decreased. Moreover, *CASP3* could be activated by $Ca^{2+}$ mediated in the ER stress pathway. Inositol 1,4,5-trisphosphate receptors (ITPRs) are responsible for $Ca^{2+}$ channel formation (Tantral et al., 2004; Mangla et al., 2020), and the upregulation of *ITPR1* and *ITPR3* indicated that *T.*

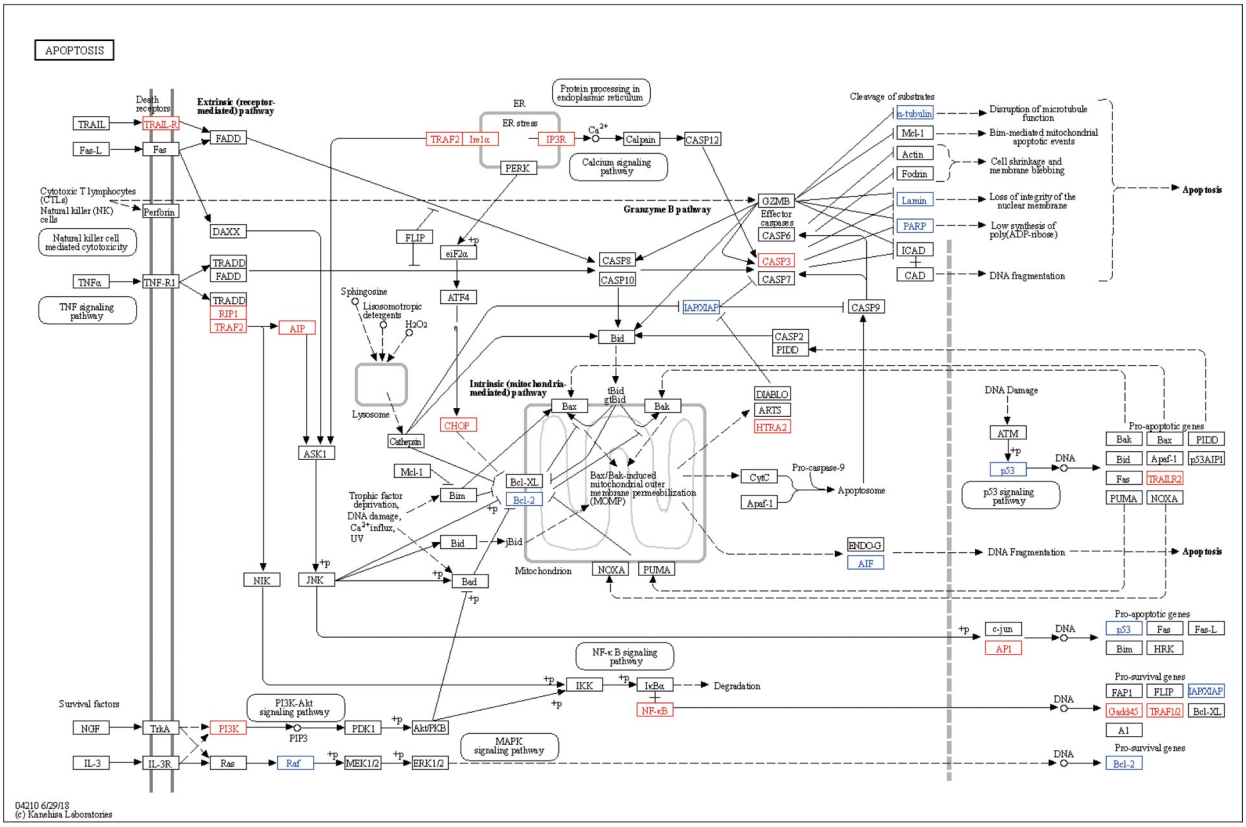


**Fig. 7 Apoptosis pathway map. The red and blue typefaces represent upregulated and downregulated genes, respectively.**

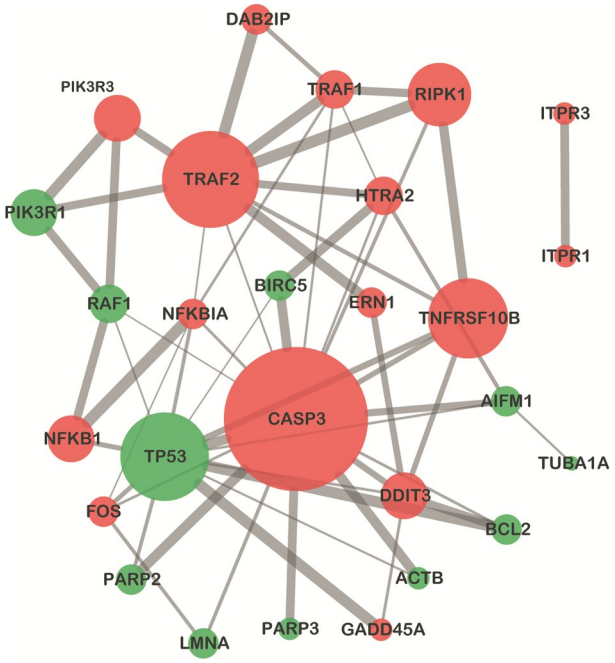


**Fig. 8 Protein–protein interaction network of DEGs enriched in the apoptosis pathway. The nodes represent DEGs, and the node size represents gene score calculated by maximal clique centrality (MCC) arithmetic. Genes with high degrees tend to be hub genes. The red and green nodes represent upregulated and downregulated genes, respectively. The edges represent proteins' association, and their thickness indicates the interaction strength of data support, including text mining, experiments, databases, co-expression, neighborhood, gene fusion, and co-occurrence. The screening threshold was set as 0.4. The top 50 pathways with corrected *P*-value of <0.05 were considered the significant pathways, and these were presented. The rich factor represents the number of DEGs that exist in this pathway accounting for the total number of genes of this pathway. DEG: differentially expressed gene.**

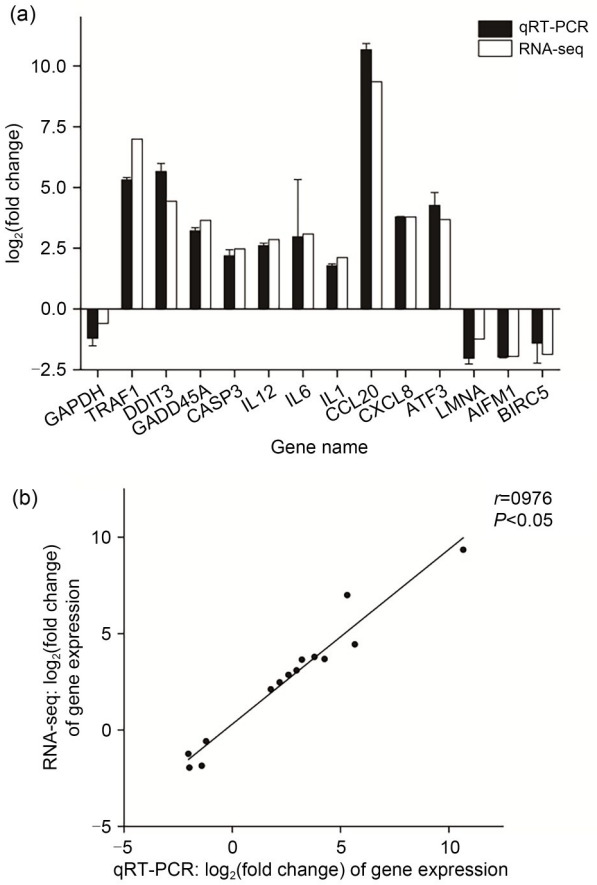


**Fig. 9 Verification of DEGs in RNA-seq data by qRT-PCR. (a) Comparison of gene expression between qRT-PCR and RNA-seq. The expression value was taken as fold change and $\log_2$-transformed. The error bar means the standard error of mean (SEM). (b) Linear correlation analysis between the expression values of qRT-PCR and RNA-seq. The correlation coefficient *r* represents the correlation between the two pieces of data, and the *P*-value means that the linear relation is statistically significant. DEG: differentially expressed gene; RNA-seq: RNA-sequencing; qRT-PCR: quantitative real-time PCR.**

*gondii* infection can also promote cellular apoptosis through this signaling pathway through the release of more $Ca^{2+}$.

The other pro-apoptosis genes, such as *DDIT3*, *GADD45A*, Fos proto-oncogene/AP-1 transcription factor subunit (*FOS*), and *HtrA2*, were also upregulated, which play roles either in cytochrome c (Cyt-C) release or IAP cleavage (Gao et al., 2009; Estaquier et al., 2012; Hu et al., 2019). However, we also observed the upregulated expression of anti-apoptosis genes such as phosphoinositide-3-kinase regulatory subunit 3 (*PIK3R3*) and NF-κB subunit 1 (*NFKB1*), and the downregulated expression of pro-apoptosis genes such as apoptosis-inducing factor mitochondria-associated 1 (*AIFM1*) and tumor protein p53 (*TP53*), which seemed contradictory to the apoptotic process. A possible explanation may be that the cell receives the invasion signal from *T. gondii* and initiates apoptosis, while the upregulation of *NFKB1* and *PIK3R3* may target the activation of immune response and autophagy or other biological processes aiming to clear the parasite at the same time. Simultaneously, the parasite can also disturb gene expression for survival and proliferation via the NF-κB and PI3K-Akt pathways (Yang et al., 2017; Ihara et al., 2020). Moreover, AIF and p53 could induce apoptosis in a caspase-independent manner (Ranjan and Iwakuma, 2016; Delavallée et al., 2020), and the downregulation of *AIFM1* and *TP53*

may imply that the caspase-independent mechanism cannot play a major role in *T. gondii*-induced apoptosis.

Herein, the apoptosis-related gene expression and pathways induced by *T. gondii* infection were analyzed systematically through transcriptomics. From the sequencing data, it was found that the *T. gondii* RH strain promoted apoptosis in Vero cells mainly by inducing the upregulation of pro-apoptosis genes and downregulation of anti-apoptosis genes, mediated by the TNF and ER stress pathways and through the ASK1-JNK pathway to disrupt mitochondrial homeostasis. Besides, *T. gondii* could act on ER to promote $Ca^{2+}$ release and disorganize the cell, which constitutes another method to induce apoptosis. It was also indicated that *T. gondii* could influence the less-studied TRAIL pathway, whose important role of apoptosis-regulation is worth further in-depth research. Overall, *T. gondii* infection is a signal for apoptosis to eliminate impaired cells and limit parasite dissemination, but the parasite can obstruct cell death to survive and propagate. Apoptotic genesis is not only associated with the strain type of the parasite but is also dependent on cell metabolism and sensitivity. Apoptosis is closely related to the cell cycle and is thus linked to immune and multiple diseases, which may be the reasons for the complexity of relevant research. Therefore, the apoptotic mechanisms between *T. gondii* and host cells need to be reconsidered and further explored.

## Data availability statement

The datasets supporting the results of this article are available in the National Center for Biotechnology Information (NCBI) Sequence Read Archive (SRA) repository with the accession number PRJNA791458.

## Acknowledgments

This research was supported by the National Natural Science Foundation of China (Nos. 81802037 and 81871684), the Qingshan Lake United Fund of Zhejiang Province (No. LQY19H190002), the Zhejiang Provincial Natural Science Foundation of China (No. LY22H190003), the Zhejiang Provincial Program for the Cultivation of High-level Innovative Health Talents, and the Basic Scientific Research Funds of Department of Education of Zhejiang Province (Nos. KYZD202104 and KYYB202101), China.

## Author contributions

Kaige DU, Fei LU, and Xunhui ZHUO performed the experimental research and data analysis. Chengzuo XIE, Haojie DING, Yu SHEN, and Yafan GAO analyzed the data. Kaige DU and Xunhui ZHUO wrote and edited the manuscript. Shaohong LU contributed to the study design and editing of the manuscript. All authors have read and approved the final manuscript, and therefore, have full access to all the data in the study and take responsibility for the integrity and security of the data.

## Compliance with ethics guidelines

Kaige DU, Fei LU, Chengzuo XIE, Haojie DING, Yu SHEN, Yafan GAO, Shaohong LU, and Xunhui ZHUO declare that they have no conflict of interest.

This article does not contain any studies with human or animal subjects performed by any of the authors.

## References

Angeloni MB, Guirelli PM, Franco PS, et al., 2013. Differential apoptosis in BeWo cells after infection with highly (RH) or moderately (ME49) virulent strains of *Toxoplasma gondii* is related to the cytokine profile secreted, the death receptor fas expression and phosphorylated ERK1/2 expression. *Placenta*, 34(11):973-982. https://doi.org/10.1016/j.placenta.2013.09.005

Ariyasu D, Yoshida H, Hasegawa Y, 2017. Endoplasmic reticulum (ER) stress and endocrine disorders. *Int J Mol Sci*, 18(2):382. https://doi.org/10.3390/ijms18020382

Bader GD, Hogue CWV, 2003. An automated method for finding molecular complexes in large protein interaction networks. *BMC Bioinformatics*, 4:2. https://doi.org/10.1186/1471-2105-4-2

Chin CH, Chen SH, Wu HH, et al., 2014. *CytoHubba*: identifying hub objects and sub-networks from complex interactome. *BMC Syst Biol*, 8(S4):S11. https://doi.org/10.1186/1752-0509-8-S4-S11

Cong W, Dottorini T, Khan F, et al., 2018. Acute *Toxoplasma gondii* infection in cats induced tissue-specific transcriptional response dominated by immune signatures. *Front Immunol*, 9:2403. https://doi.org/10.3389/fimmu.2018.02403

Cui JM, Shen B, 2020. Transcriptomic analyses reveal distinct response of porcine macrophages to *Toxoplasma gondii* infection. *Parasitol Res*, 119(6):1819-1828. https://doi.org/10.1007/s00436-020-06677-5

Delavallée L, Mathiah N, Cabon L, et al., 2020. Mitochondrial AIF loss causes metabolic reprogramming, caspase-independent cell death blockade, embryonic lethality, and perinatal hydrocephalus. *Mol Metab*, 40:101027. https://doi.org/10.1016/j.molmet.2020.101027

Enari M, Sakahira H, Yokoyama H, et al., 1998. A caspase-activated DNase that degrades DNA during apoptosis, and its inhibitor ICAD. *Nature*, 391(6662):43-50. https://doi.org/10.1038/34112

Estaquier J, Vallette F, Vayssiere JL, et al., 2012. The mitochondrial pathways of apoptosis. *In*: Scatena R, Bottoni P, Giardina B (Eds.), Advances in Mitochondrial Medicine. Springer, Dordrecht, p.157-183.

https://doi.org/10.1007/978-94-007-2869-1_7

Fox BA, Bzik DJ, 2015. Nonreplicating, cyst-defective type II *Toxoplasma gondii* vaccine strains stimulate protective immunity against acute and chronic infection. *Infect Immun*, 83(5):2148-2155. https://doi.org/10.1128/IAI.02756-14

Gao M, Guo N, Huang CS, et al., 2009. Diverse roles of GADD45α in stress signaling. *Curr Protein Pept Sci*, 10(4): 388-394. https://doi.org/10.2174/138920309788922216

Hill RD, Gouffon JS, Saxton AM, et al., 2012. Differential gene expression in mice infected with distinct *Toxoplasma* strains. *Infect Immun*, 80(3):968-974. https://doi.org/10.1128/IAI.05421-11

Hu YY, Bi Y, Yao DH, et al., 2019. Omi/HtrA2 protease associated cell apoptosis participates in blood-brain barrier dysfunction. *Front Mol Neurosci*, 12:48. https://doi.org/10.3389/fnmol.2019.00048

Ihara F, Fereig RM, Himori Y, et al., 2020. *Toxoplasma gondii* dense granule proteins 7, 14, and 15 are involved in modification and control of the immune response mediated via Nf-κB pathway. *Front Immunol*, 11:1709. https://doi.org/10.3389/fimmu.2020.01709

Kim CM, Park HH, 2020. Comparison of target recognition by TRAF1 and TRAF2. *Int J Mol Sci*, 21(8):2895. https://doi.org/10.3390/ijms21082895

Lima TS, Lodoen MB, 2019. Mechanisms of human innate immune evasion by *Toxoplasma gondii*. *Front Cell Infect Microbiol*, 9:103. https://doi.org/10.3389/fcimb.2019.00103

Lin YC, Shen ZR, Song XH, et al., 2018. Comparative transcriptomic analysis reveals adriamycin-induced apoptosis via p53 signaling pathway in retinal pigment epithelial cells. *J Zhejiang Univ-Sci B (Biomed & Biotechnol)*, 19(12):895-909. https://doi.org/10.1631/jzus.B1800408

Livak KJ, Schmittgen TD, 2001. Analysis of relative gene expression data using real-time quantitative PCR and the $2^{-\Delta\Delta C_T}$ method. *Methods*, 25(4):402-408. https://doi.org/10.1006/meth.2001.1262

Lossi L, Castagna C, Merighi A, 2018. Caspase-3 mediated cell death in the normal development of the mammalian cerebellum. *Int J Mol Sci*, 19(12):3999. https://doi.org/10.3390/ijms19123999

Lu G, Zhou J, Zhao YH, et al., 2019. Transcriptome sequencing investigated the tumor-related factors changes after *T. Gondii* infection. *Front Microbiol*, 10:181. https://doi.org/10.3389/fmicb.2019.00181

Mammari N, Halabi MA, Yaacoub S, et al., 2019. *Toxoplasma gondii* modulates the host cell responses: an overview of apoptosis pathways. *Biomed Res Int*, 2019:6152489. https://doi.org/10.1155/2019/6152489

Mangla A, Guerra MT, Nathanson MH, 2020. Type 3 inositol 1,4,5-trisphosphate receptor: a calcium channel for all seasons. *Cell Calcium*, 85:102132. https://doi.org/10.1016/j.ceca.2019.102132

Parlog A, Schlüter D, Dunay IR, 2015. *Toxoplasma gondii*-induced neuronal alterations. *Parasite Immunol*, 37(3): 159-170. https://doi.org/10.1111/pim.12157

Quan JH, Cha GH, Zhou W, et al., 2013. Involvement of PI 3 kinase/Akt-dependent Bad phosphorylation in *Toxoplasma gondii*-mediated inhibition of host cell apoptosis. *Exp Parasitol*, 133(4):462-471. https://doi.org/10.1016/j.exppara.2013.01.005

Rajedadram A, Pin KY, Ling SK, et al., 2021. Hydroxychavicol, a polyphenol from *Piper betle* leaf extract, induces cell cycle arrest and apoptosis in *TP53*-resistant HT-29 colon cancer cells. *J Zhejiang Univ-Sci B (Biomed & Biotechnol)*, 22(2):112-122. https://doi.org/10.1631/jzus.B2000446

Ranjan A, Iwakuma T, 2016. Non-canonical cell death induced by p53. *Int J Mol Sci*, 17(12):2068. https://doi.org/10.3390/ijms17122068

Rosowski EE, Saeij JPJ, 2012. *Toxoplasma gondii* clonal strains all inhibit STAT1 transcriptional activity but polymorphic effectors differentially modulate IFNγ induced gene expression and STAT1 phosphorylation. *PLoS ONE*, 7(12):e51448. https://doi.org/10.1371/journal.pone.0051448

Rosowski EE, Lu D, Julien L, et al., 2011. Strain-specific activation of the NF-κB pathway by GRA15, a novel *Toxoplasma gondii* dense granule protein. *J Exp Med*, 208(1): 195-212. https://doi.org/10.1084/jem.20100717

Sajjad N, Mir MM, Khan J, et al., 2019. Recognition of TRAIP with TRAFs: current understanding and associated diseases. *Int J Biochem Cell Biol*, 115:105589. https://doi.org/10.1016/j.biocel.2019.105589

Szklarczyk D, Franceschini A, Wyder S, et al., 2015. STRING v10: Protein–protein interaction networks, integrated over the tree of life. *Nucleic Acids Res*, 43(D1):D447-D452. https://doi.org/10.1093/nar/gku1003

Tantral L, Malathi K, Kohyama S, et al., 2004. Intracellular calcium release is required for caspase-3 and -9 activation. *Cell Biochem Funct*, 22(1):35-40. https://doi.org/10.1002/cbf.1050

Venugopal K, Marion S, 2018. Secretory organelle trafficking in *Toxoplasma gondii*: a long story for a short travel. *Int J Med Microbiol*, 308(7):751-760. https://doi.org/10.1016/j.ijmm.2018.07.007

Wan LJ, Gong LL, Wang W, et al., 2015. *T. Gondii* rhoptry protein ROP18 induces apoptosis of neural cells *via* endoplasmic reticulum stress pathway. *Parasit Vectors*, 8:554. https://doi.org/10.1186/s13071-015-1103-z

Wang T, Zhou J, Gan XF, et al., 2014. *Toxoplasma gondii* induce apoptosis of neural stem cells via endoplasmic reticulum stress pathway. *Parasitology*, 141(7):988-995. https://doi.org/10.1017/S0031182014000183

Wei W, Zhang FF, Chen H, et al., 2018. *Toxoplasma gondii* dense granule protein 15 induces apoptosis in choriocarcinoma JEG-3 cells through endoplasmic reticulum stress. *Parasit Vectors*, 11(1):251. https://doi.org/10.1186/s13071-018-2835-3

Yang ZS, Hou YH, Hao TF, et al., 2017. A human proteome array approach to identifying key host proteins targeted

by *Toxoplasma* kinase ROP18. *Mol Cell Proteomics*, 16(3): 469-484.
https://doi.org/10.1074/mcp.M116.063602

Yuan X, Gajan A, Chu Q, et al., 2018. Developing TRAIL/TRAIL death receptor-based cancer therapies. *Cancer Metastasis Rev*, 37(4):733-748.
https://doi.org/10.1007/s10555-018-9728-y

Zhou CX, Elsheikha HM, Zhou DH, et al., 2016. Dual identification and analysis of differentially expressed transcripts of porcine PK-15 cells and *Toxoplasma gondii* during *in vitro* infection. *Front Microbiol*, 7:721.
https://doi.org/10.3389/fmicb.2016.00721

Zhou LJ, Chen M, Puthiyakunnon S, et al., 2019. *Toxoplasma gondii* ROP18 inhibits human glioblastoma cell apoptosis through a mitochondrial pathway by targeting host cell P2X1. *Parasit Vectors*, 12:284.
https://doi.org/10.1186/s13071-019-3529-1

Zhuo XH, Sun HC, Huang B, et al., 2017. Evaluation of potential anti-toxoplasmosis efficiency of combined traditional herbs in a mouse model. *J Zhejiang Univ-Sci B (Biomed & Biotechnol)*, 18(6):453-461.
https://doi.org/10.1631/jzus.B1600316